

# Reproduction of the Mean, Variance, and Variogram Model in Spectral Simulation<sup>1</sup>

Tingting Yao<sup>2</sup>

---

*The application of spectral simulation is gaining acceptance because it honors the spatial distribution of petrophysical properties, such as reservoir porosity and shale volume. While it has been widely assumed that spectral simulation will reproduce the mean and variance of the important properties such as the observed net/gross ratio or global average of porosity, this paper shows the traditional way of implementing spectral simulation yields a mean and variance that deviates from the observed mean and variance. Some corrections (shift and rescale) could be applied to generate geologic models yielding the observed mean and variance; however, this correction implicitly rescales the input variogram model, so the variogram resulting from the generated cases has a higher sill than the input variogram model. Therefore, the spectral simulation algorithm cannot build geologic models honoring the desired mean, variance, and variogram model simultaneously, which is contrary to the widely accepted assumption that spectral simulation can reproduce all the target statistics. However, by using Fourier transform just once to generate values at all the cells instead of visiting each cell sequentially, spectral simulation does reproduce the observed variogram better than sequential Gaussian simulation. That is, the variograms calculated from the generated geologic models show smaller fluctuations around the target variogram. The larger the generated model size relative to the variogram range, the smaller the observed fluctuations.*

---

**KEY WORDS:** Fourier transform, Fourier coefficient, density spectrum, sequential-Gaussian simulation, fluctuation.

## INTRODUCTION

A spectral-simulation method, called Fourier Integral Method (FIM), has been proposed to generate models that will honor the spatial continuity/variogram of a modeled area  $z(u)$  in one-, two-, or three dimensions (Borgman, Taheri, and Hagan, 1984; Gutjahr, Kallay, and Wilson, 1987; McKay, 1988; Pardo-Iguzquiza and Chica-Olmo, 1993). This method is gaining acceptance because it honors the spatial continuity of petrophysical properties, such as reservoir permeability, porosity, and shale volume than do traditional sequential simulation algorithms.

---

<sup>1</sup>Received 3 June 2002; accepted 20 January 2004.

<sup>2</sup>ExxonMobil Upstream Research Company, P.O. Box 2189, Houston, Texas 77252-2189; e-mail: tingting.yao@exxonmobil.com

The spatial structure is characterized by a covariance/variogram model in the space domain and is represented by a density spectrum in the frequency domain. Distinct from the traditional sequential simulation methods such as sequential Gaussian simulation, spectral simulation is a global method in the sense that a global density spectrum is calculated once from the variogram model and the inverse Fourier transform is performed on the Fourier coefficient only once to generate a model. The advantage associated with this method is a better reproduction of the observed spatial properties. However, the widely accepted assumption that spectral simulation will reproduce the mean, variance, and variogram model of the interested properties simultaneously is not true as we will show in this paper. The theoretical background of the spectral simulation is first reviewed using 1D notations.

The spatial structure of a reservoir property  $z(u)$  is characterized by the covariance  $C_z(h)$  or variogram  $\gamma_z(h)$  in the space domain. In 1D, the covariance of  $z(u)$  is defined as the convolution product (Bracewell, 1986):

$$C_z(h) = \int_{-\infty}^{+\infty} z(u) \cdot z(u + h) du = z * \check{z}, \text{ where } \check{z}(u) = z(-u) \quad (1)$$

The Fourier transform (FT) of the covariance into the density spectrum of  $z(u)$  in the frequency domain exchanges convolution and multiplicative products:

$$s(\omega) = FT(C_z) = FT(z) \cdot FT(\check{z}) = Z(\omega) \cdot Z^*(\omega) = |Z(\omega)|^2 \quad (2)$$

where  $Z(\omega) = FT(z) = \int z(u)e^{-i\omega u} du$ , and  $Z^*(\omega)$  is the complex conjugate. The term  $s(\omega)$  is referred to as the density spectrum, the module  $|Z(\omega)|$  as the amplitude spectrum,  $Z(\omega) = |Z(\omega)|e^{-i\phi(\omega)}$  as the Fourier coefficient, and  $\phi(\omega)$  as the phase. The spectral-simulation method is based on the correspondence between the space property,  $z(u)$ , and the frequency counterparts,  $s(\omega)$  and  $\phi(\omega)$ , as illustrated in Figure 1.

In order to generate realizations of  $z(u)$ , it is sufficient to know its covariance values. The sample covariance can be estimated from the sample data of  $z(u)$ :

$$\hat{C}_z(h) = \frac{1}{N(h)} \sum_{\alpha=1}^{N(h)} z(u_\alpha) \cdot z(u_\alpha + h) - m_{z-h}m_{z+h} \quad (3)$$

where  $N(h)$  is the number of data pairs approximately separated by distance  $h$ ,  $m_{z-h} = \frac{1}{N(h)} \sum_{\alpha=1}^{N(h)} z(u_\alpha)$  is the mean of the tail values,  $m_{z+h} = \frac{1}{N(h)} \sum_{\alpha=1}^{N(h)} z(u_\alpha + h)$  is the mean of the head values.

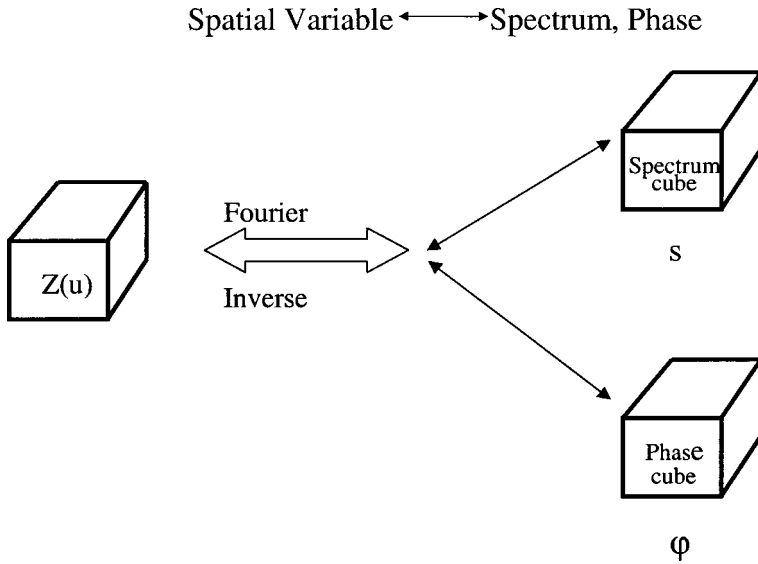


**Figure 1.** The correspondence between the space domain variable,  $z$ , and the frequency counterparts,  $s(\omega)$  and  $\varphi(\omega)$ .

Although covariance values are used in spectral simulation, the semivariogram alternative is preferred in characterizing spatial structure, which is related to covariance as:

$$\gamma_z(h) = \frac{1}{2} \int \text{Var}\{z(u+h) - z(u)\} = C_z(0) - C_z(h), \text{ if } C_z(0) \text{ exists} \quad (4)$$

where  $C_z(h)$  is the covariance, and  $C_z(0) = \text{Var}\{z(u)\}$  is the stationary variance. The sample semivariogram can be estimated as:

$$\hat{\gamma}_z(h) = \frac{1}{2N(h)} \sum_{\alpha=1}^{N(h)} (z(u_\alpha) - z(u_\alpha + h))^2 \quad (5)$$

Due to the limited number of samples available, only a few experimental variogram values,  $\hat{\gamma}_z(h_i), i = 1, \dots, n$ , can be inferred from the data. These experimental values may display large sampling fluctuations irrelevant to the underlying spatial structure. Typically, a closed-form analytical model is fitted on the variogram values to smooth out the sampling fluctuations, as well as to ensure that the corresponding covariance is positive definite. These analytical models are simply positive combinations of some basic structures which are known to be positive definite. The permissible basic variogram structures include the nugget-effect model,

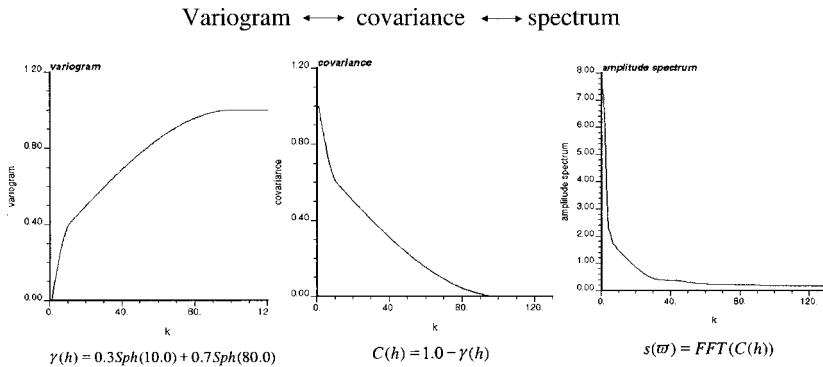


**Figure 2.** An example of the relation between the variogram, covariance, and density spectrum.

spherical model, exponential model, Gaussian model, and power model. These structures, except for the power model (which is seldom seen in reality), actually or asymptotically reach the sill  $c$ , i.e., the variance  $C_z(0)$ , at a distance called range  $a$ . For example, for the spherical model,

$$\gamma_z(h) = c \times \text{Sph} \left( \frac{h}{a} \right) = \begin{cases} c \times \left[ 1.5 \frac{h}{a} - 0.5 \left( \frac{h}{a} \right)^3 \right], & \text{if } h \leq a \\ c & \text{otherwise} \end{cases}$$

Given a variogram model, the covariance can be calculated as  $C_z(h) = C_z(0) - \gamma_z(h)$ , and the amplitude spectrum  $|Z(\omega)|$  calculated as  $\sqrt{FT(C_z)}$  per equation (2). An example of the relation between the variogram, covariance, and amplitude spectrum is given in Figure 2. Note that the variogram must attain a sill for  $C_z(h) = C_z(0) - \gamma_z(h)$  to apply, which is a nonconsequential assumption satisfied in most situations. To generate realizations through spectral simulation, simply draw phases  $\varphi(\omega)$  randomly from a uniform distribution within  $[0, 2\pi]$  and get the Fourier coefficient  $Z(\omega) = |Z(\omega)|e^{-i\varphi(\omega)}$ , the inverse Fourier transform of which provides a realization of  $z(u)$  in the space domain. This can be summarized by the following relationship:

$$\begin{array}{c} \begin{array}{c} Z \\ \uparrow \text{FFT} \\ \text{[ } |A(\omega)| \times e^{-i\varphi(\omega)} \text{]} \\ \uparrow \text{FFT}^{-1} \\ \text{Amplitude spectrum} \end{array} \quad * \quad \begin{array}{c} \check{Z} \\ \uparrow \text{FFT} \\ \text{[ } |A(\omega)| \times e^{i\varphi(\omega)} \text{]} \\ \uparrow \text{FFT}^{-1} \\ \text{Fourier coefficient} \end{array} \\ \text{phase} \end{array} = \begin{array}{c} C(h) \\ \uparrow \text{FFT} \\ s(\omega) \\ \uparrow \text{FFT}^{-1} \\ \text{Density spectrum} \end{array}$$

The implementation details will be discussed in the following section.

There are several advantages of spectral simulation over traditional geostatistical simulation. The spectral-simulation method is fast, particularly when based

on the Fast Fourier Transform (Bruguera, 1996; Kar, 1994; Lam, 1995; Mckay, 1998). It is a global method in the sense that all of the amplitude-spectrum values over the whole field,  $|Z(\omega_\nu)|$ ,  $\nu = 0, \dots, N - 1$ , are used simultaneously to generate the simulated property. Therefore, the amplitude spectrum, or variogram model in the space domain, can be honored globally over the whole field,<sup>3</sup> instead of only within search neighborhoods as with the traditional sequential-Gaussian simulation method. It is also widely believed that spectral simulation can reproduce all the target statistics—mean, variance, and variogram model, simultaneously.

Another practical advantage of using spectral simulation lies in the fact that it does not call for an analytical variogram model, as do most other simulation algorithms. The density or amplitude spectrum can be obtained either from a training image or directly from the FFT of the experimental covariance map (cube), the latter possibly previously smoothed (Yao, 1998b). In addition, conditioning to local data could be accomplished through phase identification (Yao, 1998a). Due to these advantages, spectral simulation is gaining wider application for generating stochastic realizations of random fields or geologic models for reservoir properties.

In this paper, we will first take a closer look at the properties of the discrete Fourier transform (DFT) and the implementation details of spectral simulation. Then, the issue of reproduction of the mean, variance, and variogram model in spectral simulation is discussed through both theoretical reasoning and numerical examples. Finally, we compare the ergodic fluctuation of variograms in the realizations generated from spectral simulation with those from traditional sequential-Gaussian simulation.

### REVIEW OF DISCRETE FOURIER TRANSFORM AND SPECTRAL SIMULATION

The discrete Fourier transform is the major calculation involved in spectral simulation, so it is beneficial to take a close look at properties of the discrete Fourier transform to be used in spectral simulation. For simplicity, the following notation is for the 1D case, although it can be easily extended to 2D or 3D.

Given a series of  $N$  discrete values  $f(\tau)$ ,  $\tau = 0, \dots, N - 1$ , by definition the discrete Fourier transform of  $f(\tau)$  is given by  $F(\nu)$ ,  $\nu = 0, \dots, N - 1$ , written as:

$$F(\nu) = \text{DFT}(f(\tau)) = \frac{1}{N} \sum_{\tau=0}^{N-1} f(\tau)e^{-i2\pi\tau\nu/N}. \tag{6}$$

Given the discrete transform  $F(\nu)$ , one may recover  $f(\tau)$  from the discrete inverse Fourier transform:

$$f(\tau) = \text{DFT}^{-1}(F(\nu)) = \sum_{\nu=0}^{N-1} F(\nu)e^{i2\pi\tau\nu/N}. \tag{7}$$

According to the classical spectral representation theorem, any sequence of  $N$  values  $z(h_\tau)$  with covariance  $C_z(h_\tau)$  can be expressed as a discrete inverse Fourier transform of a finite series of Fourier coefficients  $Z(\omega_\nu)$ . In 1D, that series is written as (Bracewell, 1986):

$$z(h_\tau) = \text{DFT}^{-1}(Z(\omega_\nu)) = \sum_{\nu=0}^{N-1} Z(\omega_\nu) e^{i2\pi \cdot \tau \cdot \nu / N}, \tau = 0, \dots, N - 1 \quad (8)$$

where:

$$Z(\omega_\nu) = |Z(\omega_\nu)| e^{-i\varphi(\omega_\nu)} = \sqrt{s(\omega_\nu)} e^{-i\varphi(\omega_\nu)}$$

is called the complex Fourier coefficient and  $s(\omega_\nu) = \frac{1}{N} \text{DFT}(C(h_\tau))$  (Bracewell, p. 368) is called the density spectrum.

Given a variogram model  $\gamma_z(h)$  to be honored, the spectral simulation process is as follows:

- Step 1). Use the variogram model  $\gamma_z(h)$  to calculate the discrete covariance values  $C(h_\tau)$ ,  $\tau = 0, \dots, N - 1$ , using the relation  $C(h_\tau) = C_z(h_0) - \gamma_z(h_\tau)$ , where  $C_z(h_0)$  is the covariance value at 0 lag distance,  $C_z(h_\tau)$  is the covariance value at  $h_\tau$  lag distance, and  $h_\tau = \tau \Delta h$ , with  $\Delta h$  being the cell size of the random field and  $\tau$  the number of discrete cells. The discrete Fourier transform of  $C_z(h_\tau)$  provides the discrete density spectrum  $s(\omega_\nu)$ ,  $\nu = 0, \dots, N - 1$ , whose square root provides the amplitude spectrum  $|Z(\omega)|$  per equation (2), with  $\omega_\nu = \nu \Delta \omega$ , and  $\Delta \omega = 2\pi \Delta f = 2\pi \times \frac{1}{N \Delta h}$ .
- Step 2). Randomly draw phase values  $\varphi(\omega_\nu)$ ,  $\nu = 0, \dots, N - 1$ , from a uniform distribution within  $[0, 2\pi]$ . Then, build the Fourier coefficient as  $Z(\omega_\nu) = |Z(\omega_\nu)| e^{-i\varphi(\omega_\nu)}$  in the frequency domain.
- Step 3). Perform inverse Fast Fourier transform on  $Z(\omega_\nu)$ ,  $\nu = 0, \dots, N - 1$ , to get a realization of the random field  $z(h_\tau)$ ,  $\tau = 0, \dots, N - 1$ , in the space domain.

*Note:* In order for the series  $z(h_\tau)$  to have real values in the space domain, there should be a symmetric relationship for the corresponding Fourier coefficients in the frequency domain, i.e.,  $Z(\omega_\nu) = \hat{Z}(\omega_{N-\nu})$ ,  $\nu = N/2 + 1, \dots, N - 1$ , where both  $Z(\omega_0)$  and  $Z(\omega_{N/2})$  are real values (Borgman, 1973). This, in turn, requires that  $s(\omega_\nu) = s(\omega_{N-\nu})$ , and  $\varphi(\omega_\nu) = -\varphi(\omega_{N-\nu})$  for  $\nu = N/2 + 1, \dots, N - 1$ ;  $Z(\omega_0) = |Z(\omega_0)| \cos(\varphi(\omega_0))$ ;  $Z(\omega_{N/2}) = |Z(\omega_{N/2})| \cos(\varphi(\omega_{N/2}))$ . Because the Fourier kernels satisfy the Hermitian symmetric relationship:  $e^{i2\pi \cdot \tau \cdot \nu / N} = \hat{e}^{i2\pi \cdot \tau \cdot (N-\nu) / N}$ ,  $\nu = N/2 + 1, \dots, N - 1$ , after expansion of equation (8) on  $z(h_\tau)$ , the imaginary parts cancel out and the  $N$  values  $z(h_\tau)$ ,  $\tau = 0, \dots, N - 1$ , are always real. Therefore, to generate a realization of  $N$  real values, the discrete

covariance values calculated in step 1) of the spectral simulation need only be sampled at  $C(h_\tau)$ ,  $\tau = 0, \dots, N/2$ , i.e., up to the lag distance of half the field size  $\frac{N}{2} \times \Delta h$ . The other half,  $C(h_\tau) = C(h_{N-\tau})$ ,  $\tau = N/2 + 1, \dots, N - 1$ , are mapped by the symmetric relation. Therefore, the spectral simulation can honor the covariance or variogram model only up to the half-field size  $\frac{N}{2} \times \Delta h$ . The ideal way to honor the variogram model up to distance  $N \Delta h$  is to first generate a realization of two times the field size of interest  $0, \dots, 2N - 1$ , then remove elements  $N, \dots, 2N - 1$  and only keep the part of  $0, \dots, N - 1$ . This way, the variogram model will be reproduced up to  $N \Delta h$ . This can be seen in the following numerical examples. In fact under most situations, people are only concerned about honoring the variogram model at lag distances up to the variogram range. Therefore, so long as the field size is at least twice the variogram range, spectral simulation reproduces the variogram model very well.

The discrete Fourier transform has the following properties in regards to the mean, variance, and variogram of the generated realizations through spectral simulation:

Property 1). The mean value of the generated realization is  $\mu(z) = \frac{1}{N} \sum_{\tau=0}^{N-1} z(h_\tau) = Z(\omega_0)$ , because in DFT,

$Z(\omega_0) = \frac{1}{N} \sum_{\tau=0}^{N-1} z(h_\tau) e^{-i2\pi \cdot \tau \cdot 0/N} = \frac{1}{N} \sum_{\tau=0}^{N-1} z(h_\tau)$ , no matter what the phases  $\varphi(\omega_\nu)$  are. Moreover,

$$\mu(z) = \frac{1}{N} \sum_{\tau=0}^{N-1} z(h_\tau) = Z(\omega_0) = \sqrt{s(\omega_0)} \cos(\varphi(\omega_0)) = \sqrt{\mu(C_z)} \cos(\varphi(\omega_0)) \quad (9)$$

because  $s(\omega)$  is generated from DFT of  $C_z$ .

Property 2). The variance of the generated realization is

$$\begin{aligned} \sigma^2(z) &= \frac{1}{N} \sum_{\tau=0}^{N-1} z^2(h_\tau) - \mu^2(z) = \sum_{\nu=0}^{N-1} |Z(\omega_\nu)|^2 - Z^2(\omega_0) \\ &= \sum_{\nu=0}^{N-1} s(\omega_\nu) - s(\omega_0) \cos^2(\varphi(\omega_0)) \end{aligned}$$

according to the generalized Parseval-Rayleigh theorem:  $\sum_{\tau=0}^{N-1} |f(\tau)|^2 = N \sum_{\nu=0}^{N-1} |F(\nu)|^2$  (Bracewell, p. 369). Moreover,

$$\begin{aligned} \sigma^2(z) &= \frac{1}{N} \sum_{\tau=0}^{N-1} z^2(h_\tau) - \mu^2(z) = \sum_{\nu=0}^{N-1} s(\omega_\nu) - s(\omega_0) \cos^2(\varphi(\omega_0)) \\ &= C_z(h_0) - \mu(C_z) \cos^2(\varphi(\omega_0)) \end{aligned} \quad (10)$$

according to Property 1) and  $s(\varpi)$  is calculated from the discrete Fourier transform of  $C_z(h)$ . Therefore, the variance of the generated realization  $\sigma^2(z)$  is always smaller than the target variance  $C_z(h_0)$ .

Property 3). The experimental variogram value with lag distance equal to half-field size calculated from equation (5) is

$$\begin{aligned} \gamma_z(h_{N/2}) &= \frac{1}{N/2} \sum_{\tau=0}^{N/2} (z(h_{N/2+\tau}) - z(h_\tau))^2 = 4 \sum_{v=1}^{N/4} |Z(\omega_{2v-1})|^2 \\ &= 4 \sum_{v=1}^{N/4} s(\omega_v) = C(h_0) - C(h_{N/2}) \end{aligned} \quad (11)$$

no matter what the phases are. Therefore, for different realizations, the variogram values are the same at half-field size.

The above properties in regards to mean, variance, and variogram of the generated realizations from spectral simulation can be seen from the following numerical test examples. Also, the ergodic fluctuation of variograms from multiple realizations is examined, compared with those from traditional sequential-Gaussian simulation.

### MEAN, VARIANCE, AND VARIOGRAM OF REALIZATIONS GENERATED FROM SPECTRAL SIMULATION

For any property realization generated through spectral simulation, the mean and variance of the property realization is calculated as:

$$\begin{aligned} \mu(z) &= \frac{1}{N} \sum_{\tau=0}^{N-1} z(h_\tau) = \sqrt{\mu(C_z)} \cos(\varphi(\omega_0)) \\ \sigma^2(z) &= \frac{1}{N} \sum_{\tau=0}^{N-1} z^2(h_\tau) - \mu^2(z) = C_z(h_0) - \mu(C_z) \cos^2(\varphi(\omega_0)) \end{aligned}$$

according to equations (9) and (10). The expected values of the mean and variance of multiple realizations are:

$$\begin{aligned} E\{\mu(z)\} &= \sqrt{\mu(C_z)} E\{\cos(\varphi(\omega_0))\} = 0 \\ E\{\sigma^2(z)\} &= C_z(h_0) - \mu(C_z) E\{\cos^2(\varphi(\omega_0))\} = C_z(h_0) - \frac{1}{2} \mu(C_z) \end{aligned}$$



Although the expected mean value of realizations is 0, the expected variance value is always less than the target variance  $C_z(h_0)$ .

In order to generate realizations with zero mean and variance  $C_z(h_0)$  through spectral simulation, the mean of covariance,  $\mu(C_z)$ , should be 0. Theoretically, the mean of the covariance values, i.e.,  $\mu(C_z)$  would be 0 if the generated realization has a mean value of 0. However, in an actual implementation, the covariance is calculated from a spherical or exponential variogram model using the formula  $C_z(h) = C_z(h_0) - \gamma_z(h)$ . If the variogram model has a sill value of  $C_z(h_0)$  as most always occurs, then  $C_z(h)$  calculated from variogram models are always greater than or equal to 0, so the mean value  $\mu(C_z) > 0$ . This can be seen in Figure 2: given a spherical variogram model, all covariance values are greater than or equal to 0, hence the mean of covariance values is greater than 0. Therefore, the mean value of the simulated realization can be greater or less than 0 because  $\mu(z) = \sqrt{\mu(C_z)} \cos(\varphi(\omega_0))$  with  $\varphi(\omega_0)$  being a randomly drawn angle. Moreover, the variance is less than  $C_z(h_0)$  because  $\sigma^2(z) = C_z(h_0) - \mu(C_z) \cos^2(\varphi(\omega_0))$ .

To generate realizations with zero mean value and variance equal to  $C_z(h_0)$ , we can correct the covariance before performing the Fourier transform to get the density spectrum, as follows:

1. First calculate the covariance values using equation  $C_z(h) = C_z(h_0) - \gamma_z(h)$ .
2. Calculate the mean value of the covariance  $\mu(C_z)$ .
3. Shift all covariance values by the current covariance mean value, i.e.,  $C_z^*(h) = C_z(h) - \mu(C_z)$ , so that the shifted covariance values  $C_z^*(h)$  have a zero mean. Therefore, the generated realization from spectral simulation will have zero mean, since  $\mu(z) = \sqrt{\mu(C_z^*)} \cos(\varphi(\omega_0))$ .
4. Rescale all covariance values by the ratio of  $R = C_z(h_0)/C_z^*(h_0) = C_z(h_0)/[C_z(h_0) - \mu(C_z)]$ , i.e.,  $C_z^{**}(h) = C_z^*(h) \times R$ , so that  $C_z^{**}(h_0) = C_z(h_0)$  while  $\mu(C_z^{**}) = \mu(C_z^*) \times R = 0$ . Hence the generated realization from spectral simulation will have the correct variance because  $\sigma^2(z) = C_z^*(h_0) - \sqrt{\mu(C_z^*)} \cos^2(\varphi(\omega_0)) = C_z(h_0)$ .

After the above operations, the steps described in the previous section to perform the spectral simulation will always generate realizations with exactly zero mean and the correct variance.

As a numerical example, we generated a realization with a sequence of 32 data values. Given an input spherical variogram model with a sill of 1.0 and a range of 6 cells, the mean value of the covariance is  $\mu(C_z) = \frac{1}{32} \sum_{\tau=0}^{31} C_z(h_\tau) = 0.142$  using  $C_z(h) = C_z(h_0) - \gamma_z(h)$ . The rescaling ratio is  $R = \frac{1.0}{1.0 - \mu(C_z)} = \frac{1.0}{1.0 - 0.142} = 1.165$ .

Figure 3 shows the histogram of the generated realization of 32 data values with no corrections for covariance and Figure 4 shows the histogram of the realization with correction done on the covariance before calculating the target density

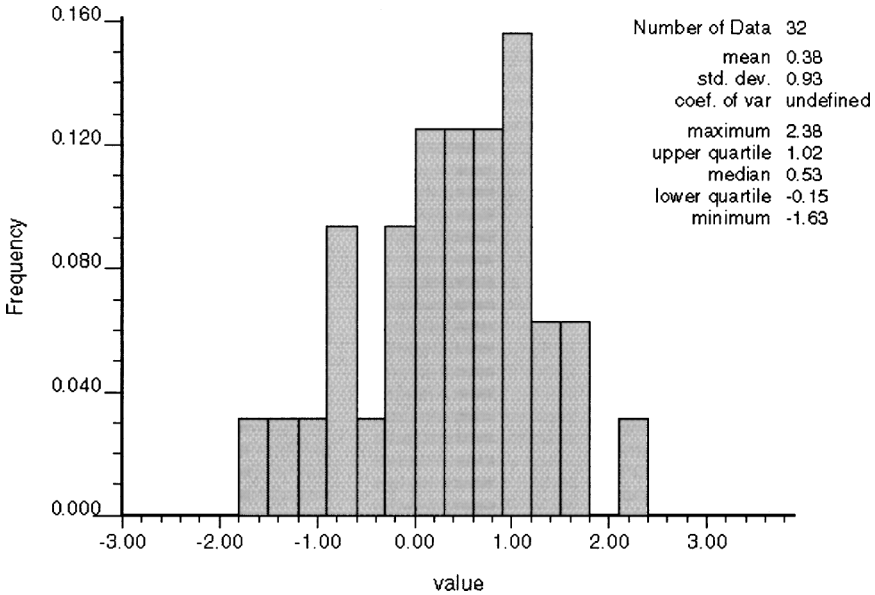


**Figure 3.** Histogram of a simulated sequence of 32 data values, without correction on covariance. Note that mean is not zero and standard deviation is not 1.0.

spectrum. Figure 3 shows the histogram of one specific realization with  $\varphi(\omega_0) = 0$ : the mean of the values in the generated realization is 0.38, which is equal to  $\sqrt{\mu(C_z)} \cos(0) = \sqrt{0.142} = 0.38$ ; the standard deviation equals 0.93, which is equal to  $\sqrt{C_z(0) - \mu(C_z) \cos^2(0)} = \sqrt{1.0 - 0.142} = 0.93$ . Figure 4 shows that the mean is zero and the standard deviation is 1.0 after correction made on covariance values before calculating the density spectrum. Moreover, we notice that the maximum value in Figure 4 is equal to the maximum value in Figure 3, shifted by  $\sqrt{\mu(C_z)}$  and rescaled by  $\sqrt{R}$ , i.e.,  $(2.38 - \sqrt{0.142}) \times \sqrt{1.165} = 2.162$ . Therefore, the generated data sequence from the corrected covariance before calculating the target spectrum is equivalent to shifting and rescaling the generated realization with no correction on the covariance, due to the linearity of the Fourier-transform operator.

Figure 5 shows the variogram calculated from the generated sequence using uncorrected (solid line) and a corrected (dashed line) covariance without assuming periodicity of the data, i.e.,  $\gamma(h) = \frac{1}{2N(h)} \sum_{\alpha=1}^{N(h)} (z(u_\alpha) - z(u_\alpha + h))^2$  where  $N(h)$  is the number of data pairs which are separated by distance  $h$ . With lag distance  $h$  increasing, fewer data pairs are found and there is more fluctuation in the calculated variogram values. Note that the variogram from the corrected covariance shows a higher sill, which is due to the rescaling of the covariance by  $R = 1.165$ . Figure 6 shows the variogram calculated from the generated sequence, assuming periodicity

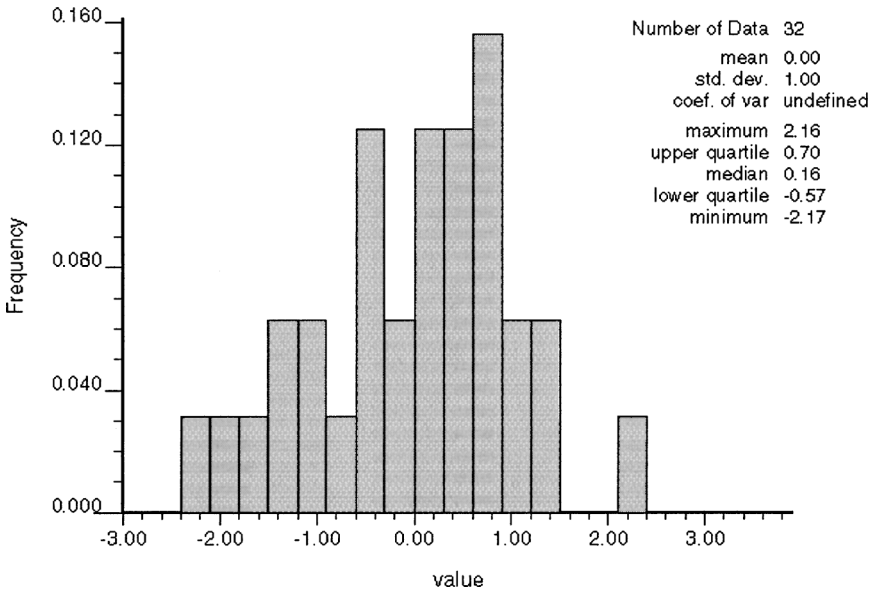


**Figure 4.** Histogram of a simulated sequence of 32 data values, with correction on covariance before calculating target density spectrum. Note that mean is exactly 0.0 and standard deviation is exactly 1.0.

of the data, i.e.,  $z(u_\alpha) = z(u_{\alpha+32})$ , as the spectral simulation algorithm does. It can be seen that the variogram calculated from the sequence without a covariance correction (solid line) exactly honors the input variogram model before the distance at 16 cells, whereas the variogram from the sequence with covariance correction (dashed line) boosts the input variogram model by the rescaling ratio,  $R = 1.165$ . Now the sill is no longer equal to  $C(0)$ , but equals  $1.165 C(0)$ . Actually, when we shifted and rescaled the covariance, we implicitly did the same to the target variogram model! Note also that, in Figure 6, the variogram values at distances beyond 16 cells are simply mapping of those values at cell distances 1–15, as we explained in the previous section.

The above example shows that the spectral simulation with covariance correction from a variogram model reproduces the mean and variance, but boosts the variogram sill. On the other hand, with no covariance correction, the spectral simulation honors the variogram model perfectly up to the half-field size, 16 cells in the example, but the mean and variance from the realization deviates from the target statistics. Therefore, in spectral simulation, either the mean and variance of the data, or the input target variogram model, can be honored, but not both! The inconsistency in this test example is significant because the variogram range is relatively long compared with the size of the field (6 vs. 32). If the size of the

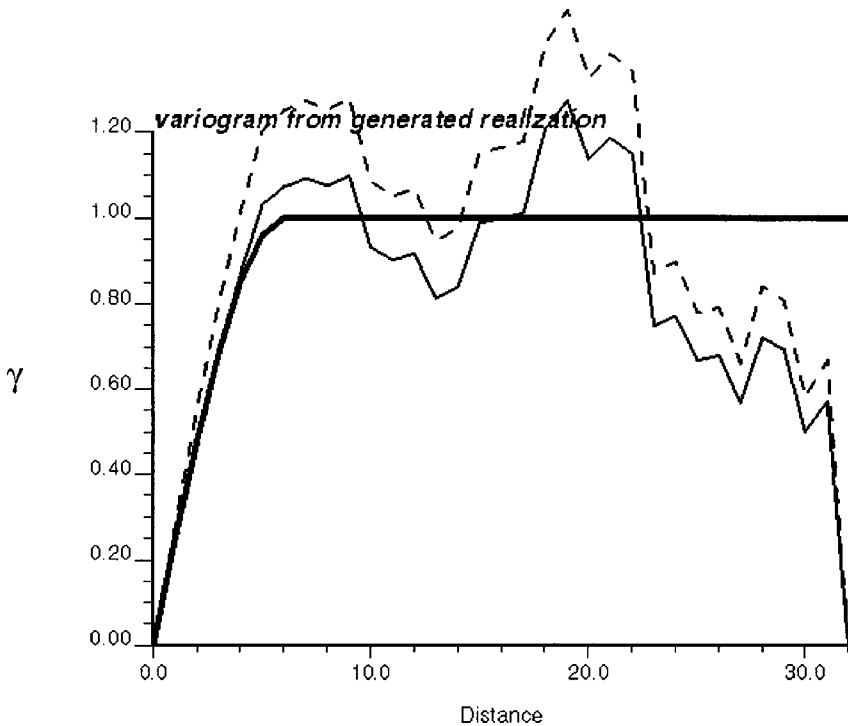


**Figure 5.** Variogram calculated only from the 32 simulated sequence data: bold line is the input variogram model with 1.0 sill and range 6 cells, fine line is from the data without covariance correction, dashed line is from the data with covariance correction. Note that the dashed line is 1.165 times the fine line.

field is much larger than the variogram range (e.g., the field size is 100 times the variogram range), then the deviation of the statistics from their target will be minimal, as shown by Pardo-Iguzquiza and Chica-Olmo (1993). In 3D situations, the mean of the covariance cube calculated from any variogram model with a reasonably not-too-long range is very close to 0 due to the contribution of lots of zero covariance values beyond the variogram range. Then, both the mean and variance, and the variogram model up to the half-field size, can be honored very well in 3D realizations.

### ERGODIC FLUCTUATION OF VARIOGRAMS: COMPARED WITH SEQUENTIAL GAUSSIAN SIMULATION

Any simulation algorithm aims at generating realizations which reproduce the target statistics, such as variogram models. “Ergodic fluctuation” refers to the

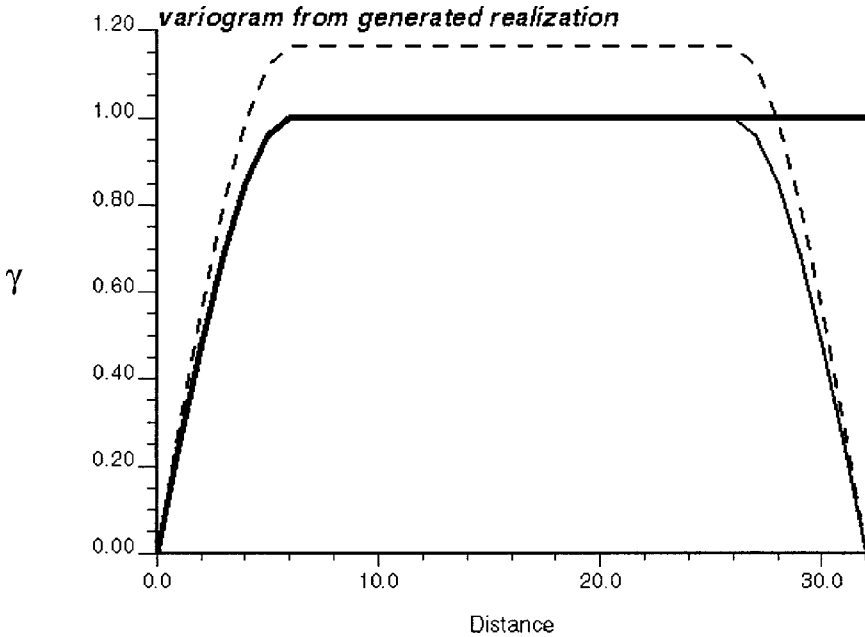


**Figure 6.** Variogram calculated from the simulated sequence data, assuming periodicity: bold line is the input variogram model with sill at 1.0 and range 6 cells, fine line is from the data without covariance correction, dashed line is from the data with covariance correction. Note: 1). The dashed line is 1.165 times the fine line. 2). The variogram is symmetric with respect to 10 lag distance, if the variogram values at distance beyond half-field size is mapped to the negative lag distance, refer to the discussion in the Introduction Section.

discrepancy between the realization statistics and the input model statistics, such as the difference between the variogram calculated from the realization and the input variogram model.

The stationary random function  $z(u)$  is said to be “ergodic” for any parameter  $\mu$  if the corresponding realization statistics  $\mu^{(l)}$  tend towards the input model statistics  $\mu$  as the size of the simulation field increases. Thus, if  $z(u)$  is stationary and ergodic and the simulation field is large enough, the statistics of any realization are expected to be exactly the same as the input model statistics. Due to its global algorithm of using the global density spectrum, spectral simulation usually generate realization showing more ergodic property.

### Ergodic Fluctuation of Varigorams With Short Range Relative to Field Size

As an example, we generate a 3D model of  $64 \times 64 \times 16$  cells with the cell spacing  $1.0 \times 1.0 \times 1.0$ . The target variogram model is spherical, anisotropic with

principal ranges 20, 10, and 5, and unit variance:

$$\gamma(|h|) = \text{Sph} \left( \sqrt{\left(\frac{h_1}{20.0}\right)^2 + \left(\frac{h_2}{10.0}\right)^2 + \left(\frac{h_3}{5.0}\right)^2} \right)$$

where  $h_1$  corresponds to the major horizontal direction of continuity, here N45E,  $h_2$  is the horizontal direction perpendicular to  $h_1$ , and  $h_3$  is the vertical direction. Using the spectral-simulation algorithm, twenty 3D realizations were generated. One realization volume and 20 variograms calculated from all realizations, with the input model shown as bold, are in Figure 7. Note that in Figure 7(B), the variogram values intersect to the value of 1.0 at a distance of 8.0, which is explained by Property (3) of the discrete Fourier transform. The calculated variograms display expected fluctuations around the input variogram model. For comparison of the ergodic fluctuation, we also apply the traditional sequential-Gaussian simulation (sgsim) method to generate 20 similar realizations. One realization and 20 variograms calculated from all realizations are shown in Figure 8. Compared

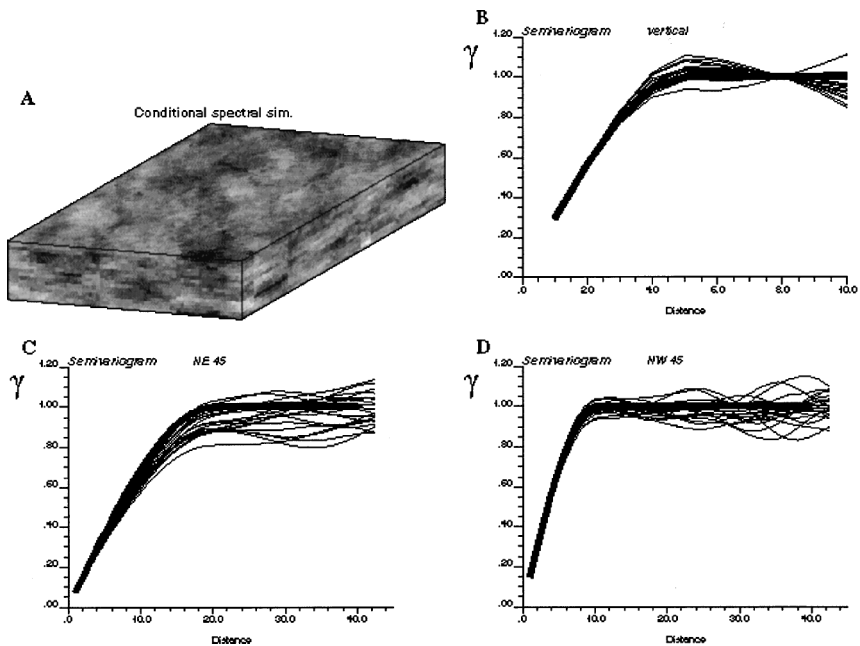


**Figure 7.** One 3D realization volume with input variogram model (bold line) and 20 simulated variograms (fine lines), using spectral simulation. (A) simulated volume; (B) simulated variogram and variogram model in the vertical direction; (C) simulated variogram and variogram model in the N45E direction; (D) simulated variogram and variogram model in the N45W direction.

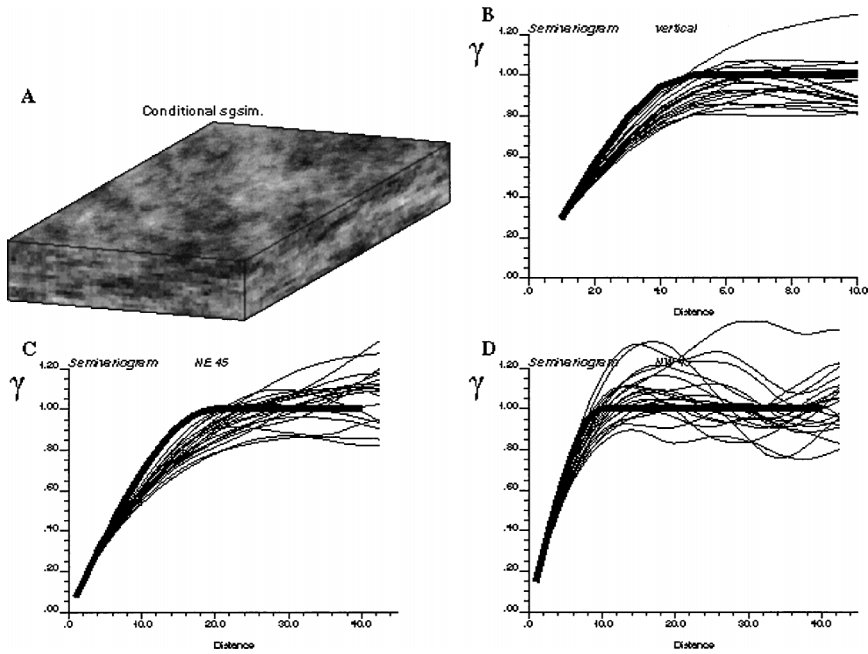


**Figure 8.** One 3D realization volume with input variogram model (bold line) and 20 simulated variograms (fine lines), using sequential Gaussian simulation. (A) simulated volume; (B) simulated variogram and variogram model in the vertical direction; (C) simulated variogram and variogram model in the N45E direction; (D) simulated variogram and variogram model in the N45W direction.

with results from spectral simulation, the variograms from models generated using sequential-Gaussian simulation fluctuate more around the input model. Theoretically, the kriging system at each cell considers correlation within the search neighborhood. However, with the simulation proceeding sequentially, more conditioning data are found within the search neighborhood of the current simulated cell. To avoid solving a huge kriging system, only a specific number of conditioning data very close to the current cell, usually no more than 48, are used in the kriging system. Therefore, in the generated realization, only variogram values at very short lag distances are reproduced.

### Ergodic Fluctuation of Variograms With Long Range Relative to Field Size

In the above example, the range of the variogram model is less than half the field size of the 3D model in the X, Y, or Z directions. The spectral-simulation algorithm shows better ergodic properties compared to the sgsim algorithm due to

the global consideration of the density spectrum, the frequency representation of variogram model.

In the following example, a model of  $64 \times 64$  cells was generated with a relatively larger variogram range, 60 cells in X direction and 5 cells in Y direction. Figure 9 shows one realization and 20 variograms calculated from 20 spectral-simulation realizations. From this, we observe: 1) At half-field location (32 cells in this case), the variogram values calculated from the spectral simulation along the X or Y direction always intersect at the same value, no matter what the random phases are. This is explained by Property (3) of the discrete Fourier transform. 2) Beyond the half-field lag distance, the target variogram model is not honored at all. On the contrary, the variograms are closely symmetric to the first half-field distance. The explanation was given in the previous section: to ensure the generated realizations are real-values, only the variogram values at half-field distance are considered. This phenomenon is dramatic here because the variogram range is relatively long compared with the field size (almost the same size as the simulation field, 60 vs. 64).

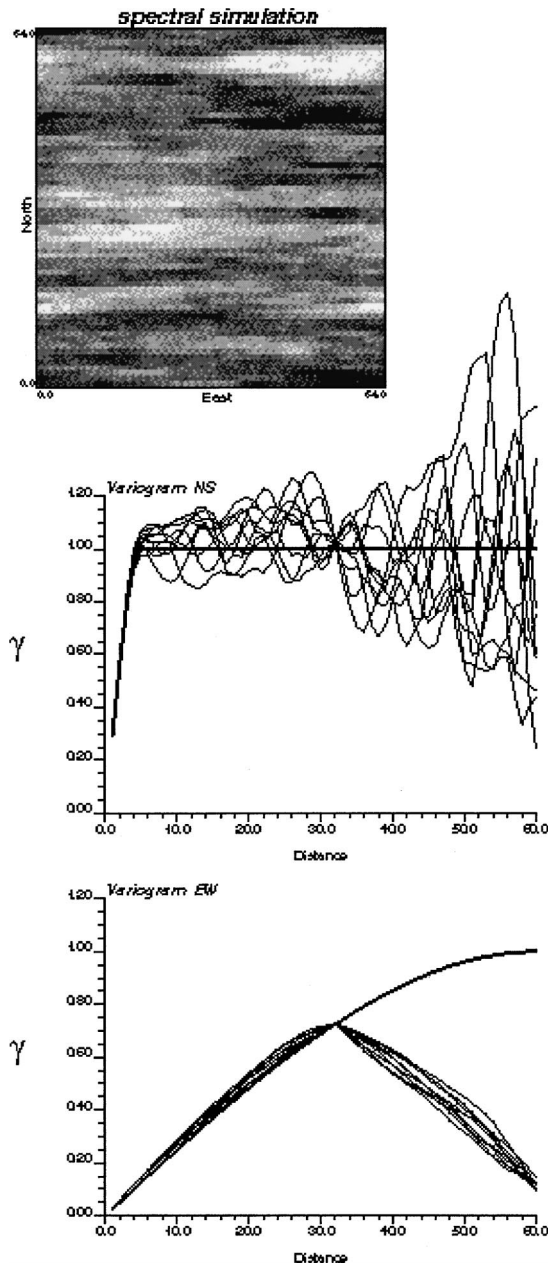
For Figure 10, we simply increased the simulated field size in the X direction by two times, so that the simulated field size is more than twice of the variogram range in the X direction. Then after spectral simulation, we cut the model back to the original size of 64 cells in the X direction. The variogram calculated from the new model honors the target very well. In fact, in order for the spectral simulation to show a good ergodic property, the ideal case would be that the simulation field size be at least twice the variogram range.

Figure 11 provides *sgsim* results for comparison. Also, we can see as the variogram range increases, the generated realizations show more fluctuations around the target variogram model. But unlike spectral simulation, this cannot be avoided by simulating a larger field.

## SUMMARY

Spectral simulation is faster than traditional sequential simulation in that it calls for only Fourier transforms instead of solving a kriging system at each simulated node. The density spectrum used in spectral simulation is obtained through a discrete Fourier transform of the covariance values, which are calculated from a given variogram model, usually with the mean value not zero. Therefore, the mean and variance of the generated realizations will deviate from the target statistics. Some correction (shift and rescale) on the covariance can be applied to generate realizations with correct mean and variance; however, this correction implicitly rescales the input variogram model, so the variogram calculated from the generated realizations has a higher sill than the input variogram model. In practice, the deviation effect will be negligible in 3D situations because the mean of the covariance cube calculated from any variogram model with a reasonably short range is near zero.





**Figure 9.** Spectral simulation with a long variogram range: one realization and 20 variograms calculated from 20 realizations in NS and EW directions vs. the input variogram model (bold line).

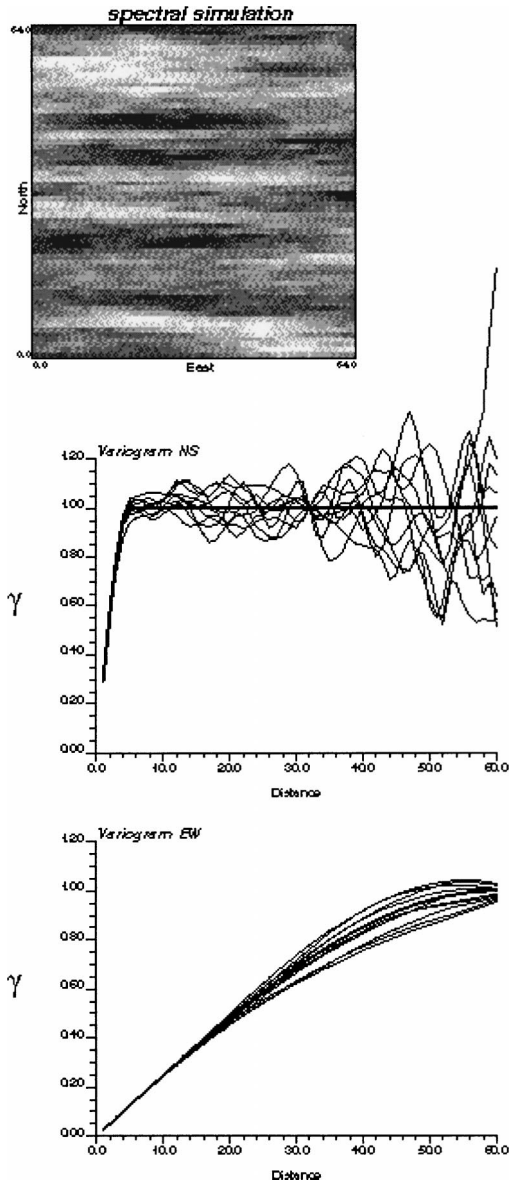


**Figure 10.** Spectral simulation with a long variogram range: one realization and 20 variograms calculated from 20 realizations in NS and EW directions vs. the input variogram model (bold line). The spectral simulation is performed on an enlarged field ( $128 \times 64$  cells). The model is then cut back to the original size ( $64 \times 64$  cells).

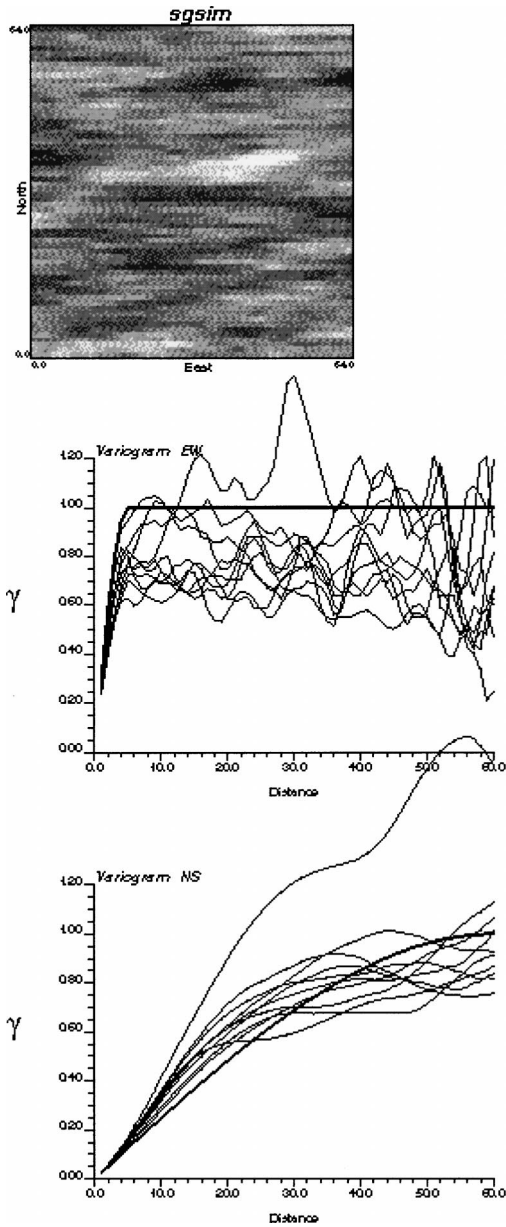


**Figure 11.** Sequential Gaussian simulation with a long variogram range: one realization and 20 variograms calculated from 20 realizations in NS and EW directions vs. the input variogram model (bold line).

Due to the symmetric relation required in spectral simulation to generate real-valued realizations, only the covariance values up to the half-field size were used. Therefore, the spectral simulation can only reproduce the input variogram model up to the half-field size. The ideal way to honor the spatial structure over the whole field is to generate realizations of twice the size of the field of interest, then cut it back to the original field size. Since traditional sequential simulation can only reproduce the spatial structure within the search neighborhood, spectral simulation has better ergodic property in regard to honoring the target variogram model in multiple realizations.

### ACKNOWLEDGMENTS

This research was done after some illuminating discussion with my colleague Glen Bishop. Tom Jones carefully reviewed the paper and provided valuable comments to help clear conceptual confusion. The author thanks the management of ExxonMobil Upstream Research Company for permitting publication of this paper.

### REFERENCES

- Borgman, L., 1973, Statistical properties of fast Fourier transform coefficients computed from real-values, covariance-stationary, periodic random sequences; research paper no. 23: Department of Statistics, University of Wyoming, Laramie, 58 p.
- Borgman, L., Taheri, M., and Hagan, R., 1984, Three-dimensional frequency-domain simulations of geological variables, *in* Verly, G., Journel, A. G., and Marechal, A., eds., *Geostatistics for natural resources characterization*, NATO ASI Series: Reidel, Dordrecht, The Netherlands, p. 517–541.
- Bracewell, R., 1986, *The Fourier transform and its application*: McGraw-Hill, Singapore, 474 p.
- Bruguera, J., 1996, Implementation of the FFT butterfly with redundant arithmetic: *IEEE Trans. Circuits Syst., Part II: Analog Digit. Signal Process.*, v. 43, no. 10, p. 717–723.
- Journel, A., and Huijbregt, C., 1978, *Mining geostatistics*: Academic Press, New York, 600 p.
- Kar, D., 1994, On the prime factor decomposition algorithm for the discrete sine transform: *IEEE Trans. Signal Process.*, v. 42, p. 3258–3260.
- Lam, K.-M., 1995, Computing the inverse DFT with the in-place, in-order prime factor FFT algorithm: *IEEE Trans. Signal Process.*, v. 43, p. 2193–2194.
- McKay, D., 1988, A fast Fourier transform method for generation of random fields, Unpublished Master's thesis: New Mexico Institute of Mining and Technology, Socorro, NM, 92 p.
- Pardo-Iguzquiza, E., and Chica-Olmo, M., 1993, The Fourier integral method: An efficient spectral method for simulation of random fields: *Math. Geol.*, v. 25, no. 4, p. 177–217.
- Yao, T., 1998a, Conditional spectral simulation with phase identification: *Math. Geol.*, v. 30, no. 3, p. 285–308.
- Yao, Y., 1998c, Automatic modeling of (cross) covariance tables using fast Fourier transform: *Math. Geol.*, v. 30, no. 6, p. 589–615.